

# Optimal generation of indistinguishable photons from non-identical artificial molecules

Emiliano Cancellieri,<sup>1,2</sup> Filippo Troiani,<sup>2</sup> and Guido Goldoni<sup>2,3</sup>

<sup>1</sup>*NEST CNR-INFM and Scuola Normale Superiore, Pisa, Italy*

<sup>2</sup>*S3 CNR-INFM, Modena, Italy*

<sup>3</sup>*Dipartimento di Fisica, Università di Modena e Reggio Emilia*

(Dated: February 21, 2024)

We show theoretically that nearly indistinguishable photons can be generated with non-identical semiconductor-based sources. The use of virtual Raman transitions and the optimization of the external driving fields increases the tolerance to spectral inhomogeneity to the meV energy range. A trade-off emerges between photon indistinguishability and efficiency in the photon-generation process. Linear (quadratic) dependence of the coincidence probability within the Hong-Ou-Mandel setup is found with respect to the dephasing (relaxation) rate in the semiconductor sources.

PACS numbers: 03.67.-a, 78.67.Hc, 42.50.-p

Single-photon sources (SPSs) are fundamental devices in quantum communication [1] and linear-optics quantum computation [2]. Essentially, a SPS consists of an atomic-like system that can be deterministically excited and thus triggered to emit single-photon wavepackets into a preferential mode. In addition, all photons have to be emitted in the same quantum state, in order to maximize the visibility of two-photon interference.

So far, single-photon generation has been demonstrated both with atomic [3, 4, 5, 6], molecular [7, 8, 9], and solid-state systems [10, 11, 12, 13, 14, 15]. Amongst the latter, self-assembled semiconductor quantum dots (SAQDs) [16] are particularly promising, for they can be controllably coupled to optical microcavities [17], so as to greatly enhance both the photon emission rate and

the collection efficiency. As a major downside, SAQDs come with a finite dispersion in terms of size, shape, and composition. This typically gives rise to spectral inhomogeneities in the meV range, *i.e.*, orders of magnitude larger than the homogeneous linewidths (few  $\mu\text{eV}$ s) of the lowest exciton transitions at cryogenic temperatures. Photons spontaneously emitted by two distinct SAQDs therefore tend to be completely distinguishable: this could impede scalability and ultimately limit the potential of semiconductor-based SPSs.

In spite of its relevance to any solid-state approach, the problem of generating indistinguishable photons with non-identical emitters has still received limited attention. In this Letter, we assess the possibility of compensating the effects of such differences between two SPSs by suitably tuning the exciting laser pulses. To this aim, we combine a density-matrix approach [18] – to simulate the system dynamics and compute the coherence functions of the emitted radiation – with a genetic algorithm [25] – to optimize the external driving fields. As a crucial point, the photon generation results from a (virtual) Raman transition. Raman transitions have already been proposed as means to avoid the classical uncertainty on the initial time of the emission process (the so-called *time-jitter*) [19, 20] and to tune both the temporal profile and the central frequency of the emitted wavepacket [5]. Here we show that such flexibility can be exploited to generate two nearly indistinguishable photons, in spite of the spectral differences between their respective semiconductor sources.

We specifically consider the case where each source is represented by two coherently coupled SAQDs (often referred to as *artificial molecule*, AM), embedded in an optical microcavity (MC) (Fig. 1). The AM is doped with an excess electron, whose levels 1 and 2 [Fig. 2(a)] define a *pseudo-spin*, corresponding to the hybridized – bonding and antibonding – states of the two dots [21, 22]; together with the lowest charged exciton states (3 and 4), these form a double  $\Lambda$ -scheme [23]. There, a Raman

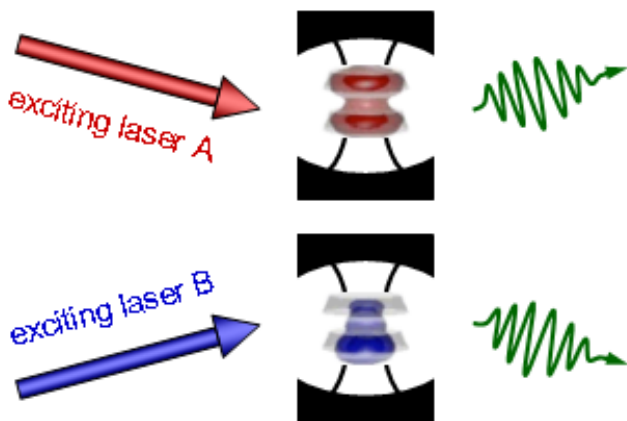


FIG. 1: (Color online) Emission scheme of indistinguishable photons from non-identical SPSs. Each source (A/B) consists of an AM (gray), doped with an excess electron (red/blue), and coupled to an optical MC (black). The effect on the photon wavepackets (green) of the differences between A and B, in terms of energies and oscillator strengths of the optical transitions, are compensated by properly tailoring the exciting laser pulses (straight arrows).

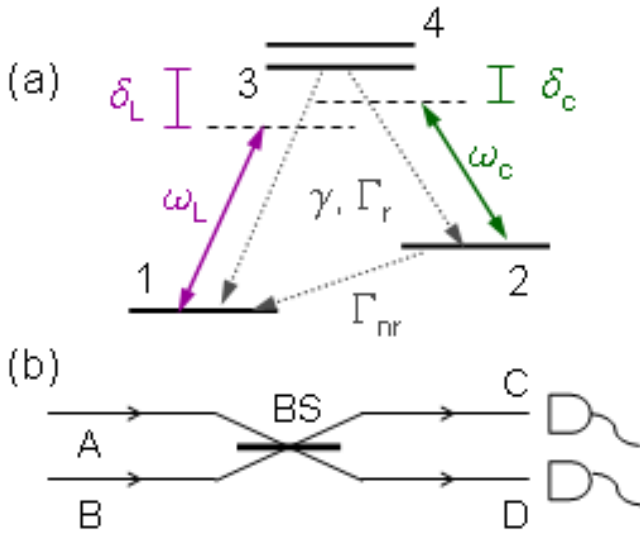


FIG. 2: (Color online) (a) Relevant level scheme for each negatively-charged AM. The levels 1 and 2 correspond to the bonding and antibonding states of the excess electron; these are optically coupled to the two lowest charged exciton states 3 and 4. The off-resonant laser pulse ( $\omega_L$ ) induces a virtual Raman transition from 1 to 2; this process results in the creation and emission of a photon from the fundamental mode of the MC ( $\omega_c$ ). (b) Schematics of the Hong-Ou-Mandel setup. The photons are emitted by the two sources A and B in the input modes of a balanced beam-splitter (BS), whose output modes are coupled to the photodetectors C and D.

transition can be induced by an off-resonant laser pulse ( $\omega_L$ ), that drives the AM from 1 to 2, while generating a cavity photon ( $\omega_c$ ).

We simulate the dynamics of the two sources (A and B) within a density-matrix approach [18]. The state of each AM-MC system is denoted by  $|j, n\rangle$ , where  $j = 1, \dots, 4$  specifies the AM eigenstate, whereas  $n$  represents the occupation number of the cavity mode. The time evolution of the density matrix within such Hilbert space is given by  $\dot{\rho} = i[\rho, H_{MC} + H_L] + \mathcal{L}\rho$  (rotating-wave approximation,  $\hbar = 1$ ). The coupling of the AM with the MC is accounted by

$$H_{MC} = \sum_{j=1,2} \sum_{k=3,4} g_{jk} (\sigma_{jk} a^\dagger + a \sigma_{jk}^\dagger), \quad (1)$$

where  $a$  is the annihilation operator of the cavity photon and  $\sigma_{jk} \equiv |j\rangle\langle k|$  the ladder operator acting on the AM state. The coupling of the AM with the exciting laser is given by

$$H_L = \frac{1}{2} \sum_{p=1}^{N_L} \sum_{j=1,2} \sum_{k=3,4} \Omega_{jk}^p(t) (e^{-i\delta_{jk}^p t} \sigma_{jk} + \text{H.c.}), \quad (2)$$

where  $\Omega_{jk}^p(t)/g_{jk} = \Omega_0^p \exp\{(t - t_0^p)^2/2\sigma_p^2\}$  gives the time envelope of the  $p$ -th laser pulse,  $\delta_{jk}^p \equiv \epsilon_k - \epsilon_j - \omega_L^p$ , and

$\epsilon_j$  the AM levels. The interaction of the AM-MC system with the environment is given by the superoperator

$$\mathcal{L} = \sum_j L(\sqrt{\gamma_j} P_j) + \sum_{j,k} L(\sqrt{\Gamma_{jk}} \sigma_{jk}) + L(\sqrt{\kappa} a), \quad (3)$$

where  $L(A)\rho \equiv (2A\rho A^\dagger - A^\dagger A\rho - \rho A^\dagger A)/2$  and  $P_j \equiv |j\rangle\langle j|$ . The three terms in Eq. 3 account for pure dephasing (with rate  $\gamma$ ), radiative ( $jk = 13, 14, 23, 24$ ) and non-radiative ( $jk = 12, 34$ ) relaxation of the AM, and cavity-photon emission, respectively. In the following, we assume for simplicity that  $\Gamma_{jk} \equiv \Gamma_r$  for all the radiative relaxation processes of the AM, and  $\Gamma_{jk} \equiv \Gamma_{nr}$  for the non-radiative ones.

The degree of indistinguishability between the photons generated by the two sources can be measured within the Hong-Ou-Mandel setup [24] [Fig. 2(b)]. There, if two indistinguishable photons enter the input ports (A and B) of a balanced beam splitter, two-photon interference results in a vanishing probability of a coincidence event ( $P_{CD} = 0$ ) in the two photodetectors at the output modes (C and D). For distinguishable photons, instead,  $P_{CD} = 1/2$ . The coincidence probability can thus be regarded as a measure of the photon indistinguishability. Formally,  $P_{CD}$  can be connected to the dynamics of the A and B sources through [19]  $P_{CD} = F_1 - F_2$ , where  $F_{p=1,2} = \kappa^2 \int dt \int d\tau f_p(t, \tau)$  and

$$f_1(t, \tau) = [n_A(t+\tau)n_B(t) + n_B(t)n_A(t+\tau)]/4, \\ f_2(t, \tau) = \text{Re} \left\{ [G_A^{(1)}(t, t+\tau)]^* G_B^{(1)}(t, t+\tau) \right\} / 2.$$

Here,  $G_\chi^{(1)}(t, t+\tau) = \langle a_\chi^\dagger(t) a_\chi(t+\tau) \rangle$  and  $n_\chi(t) = \langle a_\chi^\dagger(t) a_\chi(t) \rangle$  are, respectively, the first-order coherence function and cavity-mode occupation corresponding to the sources  $\chi = A, B$ .

In order to maximize the overlap between the wavepackets of the photons emitted by A and B, we optimize the driving laser pulses and the frequency of the cavity mode, *i.e.*, the vector  $\mathbf{X} = (\Omega_0^n, t_0^n, \sigma_n, \omega_c)$ . For two given sources [each characterized by the vector  $\mathbf{Y} = (\epsilon_j, g_{jk}, \gamma_j, \Gamma_{jk})$ , with  $\mathbf{Y}_A \neq \mathbf{Y}_B$ ], the suitability of each set of laser pulses for the generation of two indistinguishable photons is quantified by a fitness function  $\mathcal{F}(\mathbf{X}_A, \mathbf{X}_B | \mathbf{Y}_A, \mathbf{Y}_B) \geq 0$ , defined as

$$\mathcal{F} = (F_2/F_1) g(P_e^A, P_e^B). \quad (4)$$

Here,  $0 \leq F_2/F_1 \leq 1$  measures the degree of indistinguishability between the two photons, whereas  $g$  accounts for the statistics of the two SPSs; more specifically, it imposes a penalty on the vectors  $\mathbf{X}_\chi$  corresponding to a photon-emission probability  $P_e^\chi = \int n_\chi(t) dt$  far from 1. We identify the best solution ( $\mathbf{X}_\chi^0$ ) with the vectors that correspond to the maximum value of the fitness function, for the given values of the physical parameters that characterize the SPSs ( $\mathbf{Y}_\chi$ ):  $\mathcal{F}_M = \mathcal{F}(\mathbf{X}_A^0, \mathbf{X}_B^0 | \mathbf{Y}_A, \mathbf{Y}_B)$ .

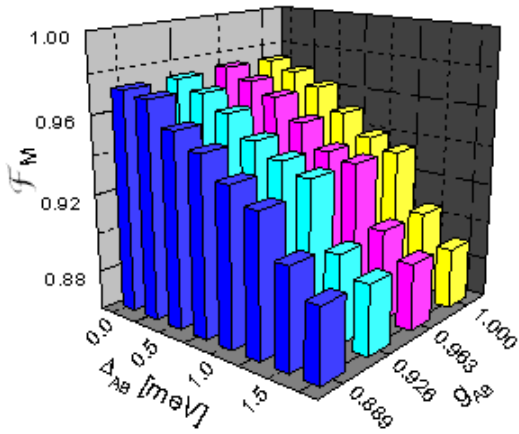


FIG. 3: (Color online) Maximized fitness function  $\mathcal{F}_M$  as a function of the differences between the A and B sources in terms of frequencies ( $\Delta_{AB} = \omega_{32}^A - \omega_{32}^B$ ) and oscillator strengths ( $g_{AB} \equiv g_{jk}^B/g_{jk}^A$ ) of the optical transitions. The remaining parameters are:  $\Gamma_{nr} = \Gamma_r^{A/B} = 10^{-3} \text{ ps}^{-1}$ ,  $\gamma_j^{A/B} = 10^{-2} \text{ ps}^{-1}$ ,  $\kappa^{A/B} = 10^{-1} \text{ ps}^{-1}$ ,  $g_{jk}^A = 0.120 \text{ meV}$ . Having found no evidence of an increased indistinguishability arising from non-gaussian laser-pulse profiles, we set here  $N_L = 1$ .

Hereafter, we take:  $g = \theta(P_e^A - P_e^t) \cdot \theta(P_e^B - P_e^t)$ , with  $\theta$  the Heaviside function. Therefore, provided that both  $P_e^A$  and  $P_e^B$  are larger than the threshold  $P_e^t$ ,  $1 - \mathcal{F}$  coincides with the coincidence probability  $P_{CD}$ , normalized to the joint emission probability of the two sources  $P_{AB} = P_e^A \cdot P_e^B = F_1$ . To this aim, we combine the density matrix approach with a genetic algorithm [25]; this allows to efficiently explore, within a large parameter space, the particularly complex landscape induced by the penalty function  $g$ .

The distinguishability between the photons emitted by the two sources mainly arises from the differences between their transition energies ( $\omega_{jk}^A \neq \omega_{jk}^B$ , being  $\omega_{jk} \equiv \epsilon_j - \epsilon_k$ ) and oscillator strengths ( $g_{jk}^A \neq g_{jk}^B$ ). In Fig. 3 we show the dependence of the maximum fitness for optimized laser pulses,  $\mathcal{F}_M$ , on  $g_{AB} \equiv g_{jk}^A/g_{jk}^B$  and  $\Delta_{AB} = \omega_{32}^A - \omega_{32}^B$  [26], for a threshold emission probability  $P_e^t = 0.9$ . The fact that  $\mathcal{F}_M < 1$  even for the case of identical sources ( $g_{AB} = 1$  and  $\Delta_{AB} = 0$ ) is due to the presence of dephasing and non-radiative relaxation (see below). By adjusting the laser pulses, moderate differences between the oscillator strengths of the two sources ( $g_{AB} \gtrsim 0.9$ ) can be efficiently compensated, whereas decreases of  $\mathcal{F}_M$  arising from mismatches between the optical-transition energies of A and B in the meV range can be limited to a few percent.

A couple of general comments are in order. On the one hand, stimulated Raman processes do increase the tolerance to inhomogeneities between the SPSs from the  $\mu\text{eV}$  – as is the case with spontaneous emission – to the meV range. On the other hand, such inhomogeneities cannot

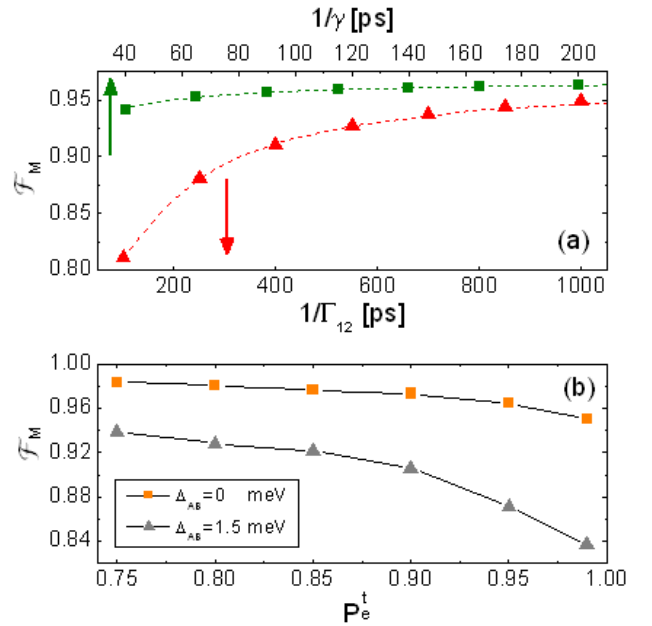


FIG. 4: (Color online) (a) Dependence of the maximum fitness function  $\mathcal{F}_M$  on the dephasing rate  $\gamma$  (upper axis, green squares) and on the non-radiative relaxation rate  $\Gamma_{21}$  (lower axis, red triangles), for  $g^{AB} = 1$  and  $\Delta_{AB} = 1.25 \text{ meV}$ . The green (red) dotted line represents the best fit of  $\mathcal{F}_M$  linear (quadratic) in  $\gamma$  ( $\Gamma_{21}$ ). (b)  $\mathcal{F}_M$  as a function of the threshold  $P_e^t$  in the photon-emission probability for  $g_{AB} = 1$ , with  $\Delta_{AB} = 0$  and  $1.5 \text{ meV}$ .

be completely compensated by properly tuning the frequencies of the driving laser pulses, as could be naively expected on the basis of a simple energy-conservation relation. These limitations are partially due to the effects of decoherence; besides, the requirement that the two sources emit photons with a high probability seems to conflict with that of maximizing their indistinguishability. In the following we investigate separately these two aspects.

The coupling between the carriers confined in each AM and the phonons gives rise to energy relaxation and dephasing. These two contributions are considered separately in Fig. 4(a), where we report  $\mathcal{F}_M$  as a function of  $\gamma$  (with  $\Gamma_{21} = 0$ , squares), and of  $\Gamma_{21}$  (with  $\gamma = 0$ , triangles), within realistic ranges of values for these rates. As in the case of two photons sequentially emitted by the same source [19], the coincidence probability increases linearly with  $\gamma$  (dotted green curve). A stronger dependence is found with respect to the non-radiative relaxation between the two lowest states in the  $\Lambda$ -scheme (a fit by a quadratic function of  $\Gamma_{21}$  is given by the dotted red line). We note, however, that the value of  $\Gamma_{21}$  can be strongly reduced by suitably engineering the AM geometry and by the application of external fields [27, 28].

In order to investigate the relation between the emission probability of the A and B photons and their in-

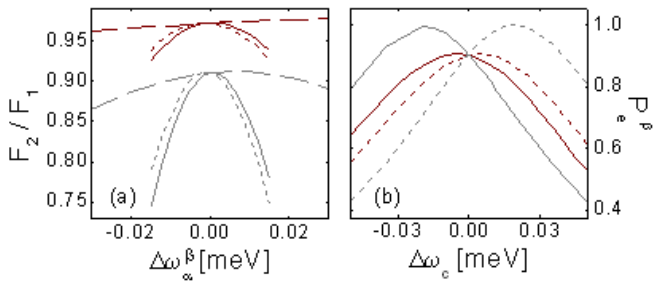


FIG. 5: (Color online) (a) Dependence of  $F_2/F_1 = 1 - P_{CD}$  on the shift of the cavity and laser frequencies from their optimized values,  $\Delta\omega_\alpha^{A/B} \equiv \omega_\alpha^{A/B} - \omega_\alpha^{A/B,0}$ , for  $\Delta_{AB} = 0$  (red) and  $\Delta_{AB} = 1.5$  meV (gray), with  $g_{AB} = 0.88$ . Solid, dashed and dotted lines correspond respectively to:  $\alpha = c$ ;  $\alpha = L$ ,  $\beta = A$ ;  $\alpha = L$ ,  $\beta = B$ . (b) Photon-emission probabilities,  $P_e^A$  (solid lines) and  $P_e^B$  (dotted), as a function of  $\Delta\omega_c$ , for  $\Delta_{AB} = 0$  (red) and  $\Delta_{AB} = 1.5$  meV (gray), with  $g_{AB} = 0.88$ .

distinguishability, we have computed  $\mathcal{F}_M$  as a function of  $P_e^t$ . In Fig. 4(b) we report two representative cases:  $\Delta_{AB} = 0$  (orange squares) and  $\Delta_{AB} = 1.5$  meV (gray triangles), with  $g_{AB} = 1$ . The photon emission probability and the degree of indistinguishability are clearly anti-correlated, thus demonstrating the existence of a trade-off between the two requirements. The dependence of  $\mathcal{F}_M$  on  $P_e^t$ , though evident even for identical sources ( $\Delta_{AB} = 0$ ), is more pronounced in the presence of a spectral mismatch ( $\Delta_{AB} = 1.5$ ). The above curves are relatively insensitive to differences in the oscillator strengths ( $g_{AB} \gtrsim 0.9$ , not shown here).

We finally comment on the robustness of the solution with respect to small departures of the control parameters from their optimal values. As a representative example, we report the dependence of  $F_2/F_1 = 1 - P_{CD}$  on the cavity frequency  $\omega_c \equiv \omega_c^A = \omega_c^B$ , referred to its optimized value  $\omega_c^0$  [Fig. 5 (a)]. The robustness of the photon indistinguishability with respect to non-optimal parameters decreases for increasing spectral mismatches between the two sources. Besides, our simulations show a stronger dependence of  $P_{CD}$  on the laser (solid and dotted lines) than on the cavity frequencies (dashed). This feature can be traced to the fact that the uncertainty on the cavity frequency ( $\sim 1/\kappa = 10$  ps) is larger than that on the laser frequency (typical duration of the optimized laser pulses are few tens of ps). As to  $P_e^{A/B}$  [Fig. 5 (b)], we note that the value corresponding to the optimized parameter ( $\Delta\omega_c = 0$ ) is close to the minimum allowed value ( $P_e^t$ ): this provides a further indication on the existence of a trade-off between photon indistinguishability and emission probability. Besides, the existence of a spectral mismatch (gray lines) makes also the fulfilment of the requirement  $P_e^A, P_e^B > P_e^t$  more sensitive to the tuning of the physical parameters. The required precision is of the order of a few  $\mu\text{eV}$  for  $\Delta_{AB} = 1.5$  meV.

In conclusion, we have investigated the degree of indis-

tinguishability between single photons emitted by non-identical artificial molecules. We found that the use of virtual Raman transitions, combined with the optimal design of the driving laser pulses, increases the tolerance with respect to the spectral inhomogeneities between the sources up to the meV energy range. Defined power-law dependences of the coincidence probability on the dephasing and (non-radiative) relaxation rates are identified. Besides, unlike the case of identical sources, a trade-off emerges between the requirements of maximizing the emission efficiency and the photon indistinguishability. It is finally worth mentioning that the use of a pseudo-spin within the  $\Lambda$ -level scheme offers promising possibilities [31]. These include the use of quantum-confined Stark effect [29] for triggering the photon emission [30], and the entangling of carrier spins localized in remote (and thus non-identical) semiconductor systems [32]. The latter goal requires the combination of a spin-photon entangling [33] process with two-photon interference within the Hong-Ou-Mandel setup.

We acknowledge financial support from the Italian MIUR under FIRB Contract No. RBIN01EY74.

- 
- [1] J. I. Cirac *et al.*, Phys. Rev. Lett. **78**, 3221 (1997).
  - [2] P. Kok *et al.*, Rev. Mod. Phys. **79**, 135 (2007).
  - [3] M. Keller *et al.*, Nature **431**, 1075 (2004).
  - [4] B. Darquié *et al.*, Science **309**, 454 (2005).
  - [5] J. McKeever *et al.*, Science **303**, 1992 (2004).
  - [6] J. Beugnon *et al.*, Nature **440**, 779 (2006).
  - [7] F. D. Martini *et al.*, Phys. Rev. Lett. **76**, 900 (1996).
  - [8] B. Lounis *et al.*, Nature **407**, 491 (2000).
  - [9] C. Brunel *et al.*, Phys. Rev. Lett. **83**, 2722 (1999).
  - [10] C. Kurtsiefer *et al.*, Phys. Rev. Lett. **85**, 290 (2000).
  - [11] P. Michler *et al.*, Nature **406**, 968 (2000).
  - [12] E. Moreau *et al.*, Phys. Rev. Lett. **87**, 183601 (2001).
  - [13] V. Zwiller *et al.*, Appl. Phys. Lett. **78**, 2476 (2001).
  - [14] C. Santori *et al.*, Phys. Rev. Lett. **86**, 1502 (2001).
  - [15] C. Santori *et al.*, Nature **419**, 594 (2002).
  - [16] A. Zrenner, J. Chem. Phys. **112**, 7790 (2000).
  - [17] A. Badolato *et al.*, Science **308**, 1158 (2005).
  - [18] M. O. Scully and M. Zubairy, in *Quantum optics* (Cambridge University Press, Cambridge, 1997).
  - [19] A. Kiraz *et al.*, Phys. Rev. A **69**, 32305 (2004).
  - [20] F. Troiani *et al.*, Phys. Rev. B **73**, 035316 (2006).
  - [21] W. Sheng *et al.*, Appl. Phys. Lett. **81**, 4449 (2002).
  - [22] G. Bester *et al.*, Phys. Rev. Lett. **93**, 47401 (2004).
  - [23] The first excited charged-exciton state 4 has to be included, for its energy separation from 3 is typically of a few meV [29], comparable to the detunings  $\delta_L$  and  $\delta_c$ .
  - [24] C. K. Hong *et al.*, Phys. Rev. Lett. **59**, 2044 (1987).
  - [25] Z. Michalewicz, in *Genetic Algorithms + Data Structures = Evolutionary Programming* (Springer-Verlag, Berlin, 1992).
  - [26] For simplicity, we keep  $\omega_{34}^A = \omega_{34}^B = 5$  meV and  $\omega_{12}^A = \omega_{12}^B = 25$  meV. Possible differences between the bonding-antibonding splittings of the two AMs can be trivially compensated by adjusting  $\omega_L^A - \omega_L^B$ .

- [27] P. Zanardi *et al.*, Phys. Rev. Lett. **81**, 4752 (1998).
- [28] A. Bertoni *et al.*, Appl. Phys. Lett. **85**, 4729 (2004).
- [29] H. J. Krenner *et al.*, Phys. Rev. Lett. **97**, 076403 (2006).
- [30] M. J. Fernée *et al.*, Phys. Rev. A **75**, 043815 (2007).
- [31] F. Troiani *et al.*, Appl. Phys. Lett. **90**, 144103 (2007).
- [32] C. Flindt *et al.*, Phys. Rev. Lett. **98**, 240501 (2007).
- [33] S. Cortez *et al.*, Phys. Rev. Lett. **89**, 207401 (2002).